SSRG International Journal of Electrical and Electronics Engineering
ISSN: 2348-8379/ https://doi.org/10.14445/23488379/IJEEE-V13I11P103

Volume 13 Issue 11, 40-52, November 2026
© 2026 Seventh Sense Research Group®

Original Article

Multi-Output Deep Learning Framework for Solar Power Forecasting and Intelligent Battery Scheduling

S.Selvi [1], K.Lakshmikhandan[2], Annamalai Muthu[3], Mohanaprakash T A[4], Neeraj Chandnani[5], Sultanuddin SJ[6]

[1]*Department of Electrical and Electronics Engineering, Panimalar Engineering College, Chennai, Tamilnadu, India.*
[2]*Department of Electrical and Electronics Engineering, Madanapalle Institute of Technology and Science, Madanapalle, Andhra Pradesh, India.*
[3]*Department of Electrical Section, College of Engineering and Technology, UTAS Nizwa, Oman.*
[4]*Department of Computer Science and Engineering, RMK Engineering College, kavaraipettai, Tamil Nadu, India.*
[5]*Department of Electronics and Communication Engineering, Koneru Lakshmaiah (KL) College of Engineering, Koneru Lakshmaiah Education Foundation (KLEF), Deemed to be University, Guntur, Andhra Pradesh, India.*
[6]*Department of Computer Science and Engineering, Vel Tech Rangarajan Dr Sagunthala R&D Institute of Science and Technology, Chennai, Tamil Nadu, India.*

[1]*Corresponding Author: selviselvarajr@gmail.com*

Received: 30 May 2026 Revised: 01 October 2026 Accepted: 30 October 2026 Published: 25 November 2026

Abstract *- The growing adoption of Solar Photovoltaic (PV) systems in modern power networks highlights the need for accurate solar-power forecasting and effective energy management to address the variability of solar generation. This study presents a multi-output deep learning framework for predicting short-term and long-term solar power and simulated battery State of Charge (SOC) to support rule-based battery scheduling. The framework evaluates three recurrent neural network architectures: Long Short-Term Memory (LSTM), Gated Recurrent Unit (GRU), and Bidirectional LSTM (BiLSTM), using solar-generation and environmental data. Solar power is predicted 15 minutes and 24 hours ahead, while SOC prediction is evaluated against a simulated reference trajectory. The forecasting framework is integrated with a rule-based scheduling strategy that determines battery charging and discharging actions according to solar generation, load demand, and specified SOC limits. Model performance is evaluated using Root Mean Square Error (RMSE) and Mean Absolute Error (MAE) over five training runs. GRU achieves the lowest RMSE and MAE for 15-minute-ahead solar-power prediction, at 2.0572 kW and 1.1733 kW, respectively. For 24-hour-ahead prediction, BiLSTM achieves the lowest RMSE and MAE, at 3.2766 kW and 2.4695 kW, respectively. For simulated SOC prediction, BiLSTM achieves the lowest RMSE of 5.1630 percentage points, whereas LSTM achieves the lowest MAE of 3.5434 percentage points. These results indicate that the best-performing architecture depends on the prediction target and evaluation metric. The framework provides a unified approach to multi-horizon solar-power forecasting, simulated SOC estimation, and rule-based battery scheduling. Further validation using measured battery data and quantitative energy-management indicators is required to establish its practical impact on grid-energy imports, operating costs, and system efficiency.*

Keywords *- Intelligent battery scheduling, BiLSTM, Deep learning, Renewable energy management, Solar power forecasting.*

1. Introduction

Solar PV (PV) generation has become a key driver in the transition to cleaner and more sustainable electricity generation when it comes to large-scale integration of PV in modern power systems. When it comes to large-scale, PV is a key driver in the transition to cleaner and more sustainable electricity generation in modern power systems.

However, due to these benefits, the intermittency of solar resources also means there is forecasting uncertainty, and accurate forecast and intelligent energy management are critical for reliable operation of the systems. Predictive solar power generation forecasts can also prove useful for better planning, power balancing, and efficient operation of renewable energy systems [1, 2].

With the latest developments in AI, machine learning and deep learning have become prevalent methods used for solar forecasting. These methods can learn from historical time-series data to capture complex nonlinear patterns and temporal relationships, which are not possible in traditional statistical methods. The behaviour of solar irradiance changes very quickly with changing weather conditions, and traditional forecasting methods like Autoregressive Integrated Moving

This is an open access article under the CC BY-NC-ND license (http://creativecommons.org/licenses/by-nc-nd/4.0/)

Average (ARIMA) is not effective in capturing this behaviour. LSTM networks are widely used for PV forecasting because their memory mechanism allows relevant information from earlier observations to be retained.

The increasing use of solar Photovoltaic (PV) systems has created new opportunities for low-carbon electricity generation. However, PV output is strongly influenced by changes in irradiance, temperature, and time-dependent operating conditions. These variations introduce uncertainty into power-system operation and make reliable PV generation forecasting important for energy planning and management.

Several studies have investigated deep learning approaches for solar power forecasting. LSTM-based models have been applied to short-term solar forecasting [6, 7], while GRU-based models have also been explored because of their relatively simple architecture. Hybrid and ensemble learning approaches have been investigated to improve forecasting performance [8, 9]. Although these methods have contributed to the development of PV forecasting, improving prediction accuracy alone does not establish how forecasts can be used to support battery operation and energy management.

Metaheuristic optimization techniques have also been investigated for PV forecasting and energy management. Particle Swarm Optimization (PSO) and Genetic Algorithms (GA) can be used to search for suitable model parameters or optimization configurations.

For example, Zhen et al. [10] developed a GA-optimized BiLSTM model for PV power forecasting, demonstrating the application of evolutionary optimization to recurrent neural networks. PSO-based methods have also been considered in battery energy scheduling [11].

Although optimization-based methods can support forecasting or scheduling objectives, they may introduce additional computational requirements. Furthermore, optimizing PV forecasting and optimizing battery operation are distinct tasks, and neither alone establishes the effectiveness of a framework that jointly predicts solar power and battery State of Charge (SOC).

Transformer-based models have also attracted attention because attention mechanisms can capture long-range dependencies in time-series data. However, the computational requirements and data needs of complex architectures may affect their suitability for some real-time energy management applications.

The selection of an appropriate forecasting model therefore depends on the prediction task, available data, and computational constraints. In this study, LSTM, GRU, and BiLSTM models are evaluated within a common multi-output forecasting framework rather than assuming that a single architecture is universally superior [8, 9, 20, 21].

Battery Energy Storage Systems (BESS) help address solar power variability by storing surplus energy during periods of high generation and supplying energy when generation is insufficient [11, 12]. Forecasting errors can affect charging and discharging decisions and may contribute to energy losses or unnecessary battery cycling [12, 13]. Integrating forecasting with battery management can therefore provide information for coordinating PV generation, battery SOC, and energy demand. However, the benefits of such integration need to be evaluated using appropriate battery-management indicators rather than inferred from forecasting accuracy alone.

Multi-output learning enables related variables to be predicted within a shared modelling framework. Previous studies have investigated deep learning-based multi-output quantile forecasting of PV generation [16] and physics-informed machine learning for hourly multi-output solar forecasting [17].

These studies demonstrate the potential of multi-output approaches for solar forecasting. In a PV-battery system, predicting solar power at different horizons alongside battery SOC may provide useful information for subsequent scheduling decisions.

Forecasting and control are both important in smart grids and autonomous energy systems. Previous research has investigated predictive management for PV-battery systems, intelligent energy management in PV-wind-battery microgrids, and model predictive control for microgrid operation [12, 14, 15]. These approaches demonstrate the relevance of integrating prediction and energy management, although their system configurations and objectives differ from the framework investigated in this study.

Table 1 summarizes selected studies on PV forecasting and energy management according to their modelling approaches, forecasting objectives, and treatment of battery storage. The reviewed literature includes recurrent neural networks, hybrid deep learning, metaheuristic optimization, multi-output forecasting, and Transformer-based approaches. This comparison highlights the range of existing methods and the distinction between forecasting-focused studies and approaches that also consider battery management. To address this gap, this study presents a multi-output deep learning framework that predicts 15-minute-ahead PV power, 24-hour-ahead PV power, and simulated battery SOC using LSTM, GRU, and BiLSTM models. The predicted outputs are linked to a rule-based battery scheduling strategy. The study compares the forecasting performance of the three architectures across the prediction targets and examines the contribution of selected input features. Since the SOC

reference is simulated rather than measured from a physical battery, the results assess prediction performance against the specified simulation and demonstrate the implementation of the scheduling rules;

Table 1. Comparison of representative solar forecasting and energy-management approaches

Reference	Approach / Model	Primary Application	Battery/SOC Integration	Research Gap/ Limitation
[6]	Probabilistic PV forecasting	Day-ahead PV generation	No joint SOC scheduling	Forecast uncertainty and PV prediction are the main focus.
[7]	LSTM and Random Forest	Solar-plant energy forecasting	No	Predicts PV generation without joint SOC prediction and scheduling.
[8]	Hybrid deep-learning models	Solar-power time-series forecasting	No	Focuses on forecasting-model performance.
[9]	PV forecasting review and case studies	Short-term PV forecasting	Not the main focus	Reviews forecasting methods rather than a unified forecasting-scheduling framework.
[10]	GA-optimized BiLSTM	Ultra-short-term PV forecasting	No joint SOC scheduling	Optimizes the forecasting model but does not jointly address SOC scheduling.
[11]	TCN-ECANet-GRU	Short-term PV forecasting	No	Uses a hybrid forecasting architecture without joint SOC prediction.
[12]	Predictive PV-battery management	PV-battery energy management	Yes	Studies predictive management but not the same multi-output forecasting formulation.
[14]	Intelligent prediction with energy-management strategy	PV-wind-battery microgrid	Yes	Integrates prediction and management in a microgrid setting, with a different system formulation.
[15]	Model predictive control	Microgrid operation optimization	Yes	Optimizes microgrid operation rather than jointly forecasting PV horizons and SOC.
[16]	Multi-output quantile forecasting	PV generation forecasting	No joint battery scheduling	Focuses on probabilistic multi-output forecasts.
[17]	Physics-informed machine learning	Hourly multi-output solar forecasting	No joint SOC scheduling	Uses physics-informed forecasting without the same SOC-based scheduling integration.
[18]	Hybrid deep learning with transfer learning	Short-term PV forecasting	No	Uses transfer learning for forecasting but does not integrate SOC scheduling.
[19]	Autoformer	Long-term time-series forecasting	No	General time-series forecasting architecture, not a PV-battery management framework.
[20]	Informer	Long-sequence time-series forecasting	No	Forecasting-focused architecture without joint SOC prediction and scheduling.
[21]	Transformer-variant PTFNet	Day-ahead PV forecasting	No	Addresses PV forecasting without joint SOC prediction and battery scheduling.
Proposed work	Multi-output LSTM, GRU, and BiLSTM	15-minute-ahead and 24-hour-ahead PV power; simulated SOC	Yes-rule-based scheduling	Integrates multi-output forecasting and simulated SOC prediction with rule-based scheduling.

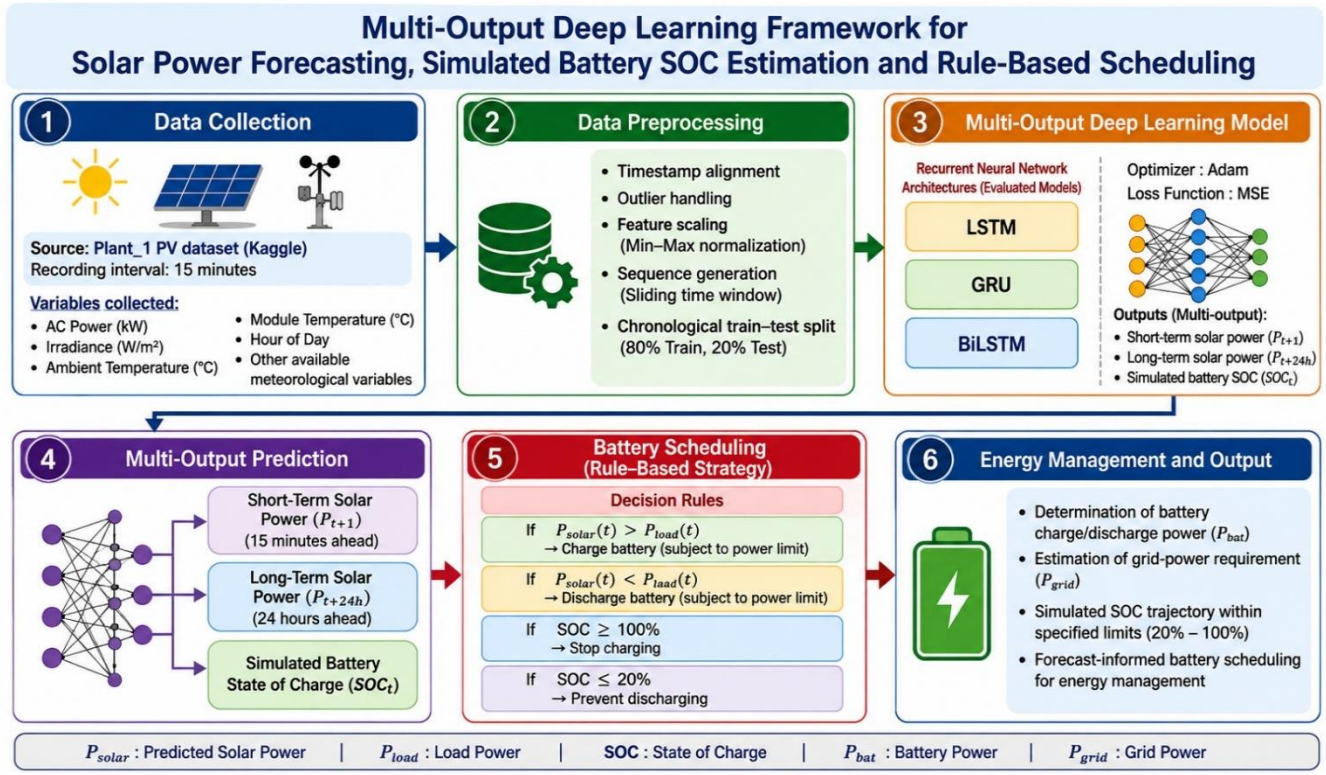

Fig 1. Proposed multi-output deep learning framework illustrating data collection, preprocessing, forecasting, multi-output prediction, battery scheduling, and energy management.

They do not, by themselves, establish reductions in grid-energy imports, operating costs, or battery degradation. The main contributions of this study are as follows:

1. A multi-output recurrent forecasting framework is developed to predict 15-minute-ahead PV power, 24-hour-ahead PV power, and simulated battery State of Charge (SOC) simultaneously.
2. The forecasting outputs are linked to an SOC-based, rule-based battery scheduling strategy, connecting prediction with subsequent energy-management decisions.
3. LSTM, GRU, and BiLSTM architectures are comparatively evaluated using five independent training runs to assess predictive performance and variability.
4. A feature-removal ablation study is conducted to examine the effects of AC power, weather variables, and time information on the different prediction targets.
5. The framework integrates multi-horizon PV forecasting, simulated SOC prediction, and rule-based battery scheduling using recurrent neural network architectures.

The novelty of this study does not lie in introducing a new recurrent architecture or a new battery optimization algorithm. Rather, its contribution lies in integrating multi-output PV forecasting, simulated SOC prediction, and rule-based battery scheduling within a common framework, as shown in Figure 1.

This approach provides a structured way to connect multiple forecasting tasks with battery scheduling decisions while retaining relatively simple LSTM, GRU, and BiLSTM model architectures.

2. Materials and Methods

2.1. Dataset Description

The dataset was sampled at 15-minute intervals and consisted of synchronized solar-generation and weather measurements. The generation data included time-series measurements of AC power P_{AC}, representing the electrical power generated by the PV system.

The weather data included the environmental variables listed in Table 2. The generation dataset contained measurements from 22 source/inverter units. Since multiple measurements were recorded at the same timestamp, the AC-power measurements were aggregated across the source units to obtain the total plant-level AC power.

The aggregated generation data were then synchronized with the weather measurements using the common timestamp. After aggregation and synchronization, 3,157 observations were obtained for the period from 15 May 2020 to 17 June 2020**.** The final dataset contained no missing observations.

Table 2. Input features

Variable	Unit	Description
AC Power P_{AC}	kW	Electrical power generated by the PV system
Irradiance	W/m²	Solar radiation incident on the PV panels
Ambient Temperature	°C	Atmospheric temperature
Module Temperature	°C	Temperature of the PV modules
Hour	h	Hour of the day representing the daily temporal variation in solar generation

A sliding window containing 24-time steps was used to construct the input sequences. Since the measurements were recorded at 15-minute intervals, each input sequence represents the preceding 6 hours of system operation. These input sequences were used to predict solar power 15 minutes ahead, solar power 24 hours ahead, and the simulated reference battery SOC. Min-Max normalization was applied to the input variables. The normalization parameters were fitted using only the training data and subsequently applied to the testing data to reduce the risk of data leakage.

2.2. Feature Definition

The input feature vector at time step t is defined as in Equation 1

$$X_t = [G_t, T_{a,t}, T_{m,t}, P_{ACt}, H_t] \quad (1)$$

represent AC power, irradiance, ambient temperature, module temperature, and hour of the day, respectively. These variables were selected because they were available throughout the dataset and represent the main electrical, environmental, and temporal conditions associated with PV generation. Humidity, cloud cover, precipitation, soiling effects, and long-term panel degradation were not included because corresponding measurements were not available in the dataset. The absence of these variables may introduce additional uncertainty under rapidly changing weather conditions or long-term changes in PV performance. Their inclusion can be investigated in future studies when suitable measurements are available.

The target output vector is represented in Equation 2.

$$Y = [P_{t+1}, P_{t+24h}.SOC_t] \quad (2)$$

where P_{t+1} denotes the 15-minute-ahead solar-power prediction and P_{t+24h} denote 24-hour-ahead solar power prediction, while SOCt represents the battery state of charge.

2.3. Deep Learning Model Selection

LSTM, GRU, and BiLSTM models were selected for solar-power forecasting because of their ability to model nonlinear temporal relationships in sequential data. LSTM networks are designed to retain relevant information over extended sequences, while GRU networks use a simpler gating structure with fewer parameters. BiLSTM networks process the available historical sequence in both directions, allowing the model to capture temporal relationships between earlier and later positions within the input sequence.

The three forecasting models were implemented using the same input features, sequence length, output structure, and training procedure to provide a consistent comparison. The LSTM model consists of one LSTM layer with 64 units followed by a fully connected Dense layer with three output neurons. The GRU model consists of one GRU layer with 64 units followed by the same three-neuron Dense output layer. The BiLSTM model consists of one bidirectional LSTM layer with 64 units in each direction, followed by a Dense layer with three output neurons. All three models use the same 24-time-step input sequence and the same five input features. The larger parameter counts of the BiLSTM model results from its forward and backward recurrent branches rather than from the use of additional stacked layers.

For the stated five-feature input and three-output architecture, the corresponding trainable parameter counts are 18,115 for LSTM, 13,635 for GRU, and 36,227 for BiLSTM. These differences reflect the number of recurrent gates and the bidirectional structure of the models.

For the BiLSTM model, the forward and backward hidden states can be represented as is given in Equation 3-5.

$$\overrightarrow{h_t} = LSTM_f(x_t, \overrightarrow{h_{t-1}}) \quad (3)$$

$$\overleftarrow{h_t} = LSTM_b(x_t, \overleftarrow{h_{t+1}}) \quad (4)$$

and the resulting representation is obtained by combining the two directional hidden states:

$$h_t = \{\overrightarrow{h_t}; \overleftarrow{h_t}\} \quad (5)$$

$\overrightarrow{h_t}$ denote the forward and $\overleftarrow{h_t}$ backward hidden states, respectively, and denotes their concatenation. By processing the observations in both directions within the historical input sequence, the BiLSTM model can represent relationships between earlier and later positions in the available 24-time-step window.

The models were implemented using Python and TensorFlow/Keras in the Kaggle notebook environment. The

hyperparameters were selected based on convergence behaviour, forecasting stability, and computational requirements observed during preliminary experiments. The training settings are listed in Table 3.

Table 3. Hyperparameter settings used for model training

Training Parameter	Selected Setting
Optimization algorithm	Adam
Learning rate	Adam default learning rate
Mini-batch size	32
Training epochs	20
Input sequence length	24 time steps
Number of recurrent units	64
Dropout probability	Not used
Recurrent activation	Model default activation
Output layer activation	Linear
Objective function	Mean Squared Error (MSE)

The 24-time-step input represents the preceding 6 hours because the dataset was sampled at 15-minute intervals. The use of the same input sequence and training settings for all three architectures allows their forecasting performance to be compared under consistent experimental conditions.

2.4. Multi-Output Prediction

The trained recurrent models simultaneously predict three outputs: short-term solar power, 24-hour-ahead solar power, and simulated battery State of Charge (SOC).

This multi-output formulation enables the models to learn the three prediction tasks from the same historical input sequence and provides forecasting information for subsequent rule-based battery scheduling.

The predicted SOC is evaluated against a simulated reference trajectory generated using the specified battery simulation assumptions; it does not represent measured SOC from a physical battery.

2.5. Loss Function

The model is optimized using a combined Mean Squared Error loss function that minimizes prediction errors across all output variables.

$$L = \frac{1}{N}\sum_{i=1}^{N}[(P_{t+1} - \hat{P}_{t+1})^2 + (P_{t+24} - \hat{P}_{t+24})^2 + (SOC_t - \hat{SOC}_t)^2] \quad (6)$$

2.6. Battery SOC Model

The battery State of Charge (SOC) is updated based on the energy balance between solar generation and load demand. A rule-based scheduling strategy determines the charging and discharging actions according to the difference between solar power and load demand, subject to the specified battery operating limits.

The simulated battery SOC is calculated as

$$SOC_{t+1} = clip(soc_t + \frac{100\,\Delta t}{E_{bat}}\left[\eta_c P_{ch,t} - \frac{P_{dis,t}}{\eta_d}\right] SOC_{\min}, SOC_{\max}) \quad (7)$$

The charging and discharging powers are determined as follows:

$$P_{ch,t} = min(\,max(\,P_{solar,t} - P_{load}, 0)P_{ch,max} \quad (8)$$

$$P_{dis,t} = min(\,max(\,P_{load} - P_{solar.t}, 0)P_{dis,max} \quad (9)$$

- Charge if P solar > Pload, subject to the charging power limit and maximum SOC of 100%
- Discharge if Psolar< Pload, subject to the discharging power limit and minimum SOC of 20%
- Stop charging if $SOC \geq 100$
- Prevent discharge if $SOC \leq 20$

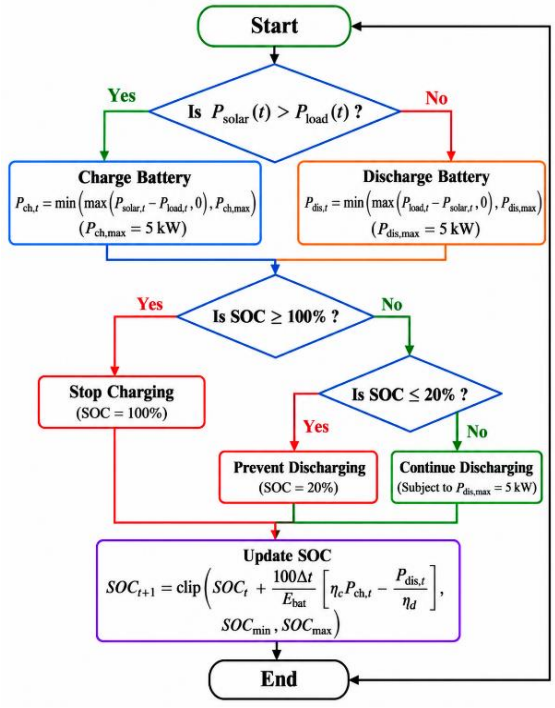

Fig 2. Battery scheduling strategy

Figure 2 illustrates the rule-based battery scheduling strategy. The controller compares solar generation with load demand to determine the charging or discharging action, applies the 5 kW power limits, and updates the simulated SOC within the specified operating range. This strategy provides a simple control mechanism for battery scheduling using solar generation and load demand.

Optimization-based methods, model predictive control, and reinforcement learning can support more advanced battery-management decisions but generally require additional system constraints, optimization procedures, or

training. A detailed comparative evaluation of these approaches is beyond the scope of this study.

2.7. Grid-Energy Objective

The system aims to minimize grid power usage by efficiently utilizing predicted solar energy and battery storage, as given by Equation 10.

$$J = \sum_{t=1}^{T} Pgrid\ (t) \quad (10)$$

Where J is the total grid energy consumption and Pgrid (t) is the grid power usage

2.8. Performance Metrics

Root Mean Square Error (RMSE) and Mean Absolute Error (MAE) were used to assess the performance of the proposed models. RMSE measures the overall prediction error, with larger errors receiving greater weight than smaller errors, while MAE measures the average absolute difference between the predicted and reference values in the same units as the variable being predicted [21].

The RMSE and MAE values were calculated for each output variable. To assess the consistency of model performance, the models were trained repeatedly using different random seeds, and the results were reported using the mean, Standard Deviation (SD), and 95% Confidence Interval (CI). MAPE was not included because solar-power values approach zero during periods of low or no solar generation, which can result in unstable or disproportionately large percentage errors.

2.9. Feature-based Ablation Study

A feature-based ablation study was conducted using the BiLSTM architecture to examine the contribution of the principal input variables. Four input configurations were evaluated: (i) the full feature set containing AC power, irradiance, ambient temperature, module temperature, and hour of day; (ii) AC power and hour of day, excluding the weather variables; (iii) AC power and weather variables, excluding the time feature; and (iv) AC power alone. The same sequence length, model architecture, training procedure, chronological data partitioning, and evaluation protocol were used for all configurations. Each configuration was evaluated over five runs with different random seeds.

2.10. Methodological Considerations and Reproducibility

For a fair comparison, the LSTM, GRU, and BiLSTM models were developed using the same input features, sequence length, output structure, data partitioning method, and loss function. The input sequence contained 24 historical time steps, corresponding to a six-hour observation window at 15-minute intervals. The output layer produced three predictions: solar power 15 minutes ahead, solar power 24 hours ahead, and simulated battery State of Charge (SOC). The normalization parameters were fitted exclusively using the training data and subsequently applied to the testing data. This procedure was followed to maintain consistency among the models and reduce the possibility of information leakage during model development and evaluation. Model performance was assessed using Root Mean Square Error (RMSE) and Mean Absolute Error (MAE), with the mean, standard deviation, and 95% confidence interval calculated across five training runs.

Table 4. Repeated-Run forecasting performance of the evaluated models

Model	Output	RMSE (Mean ± SD)	RMSE 95% CI	MAE (Mean ± SD)	MAE 95% CI Half width
LSTM	P_{t+1}	2.2183 ± 0.0630 kW	± 0.0782 kW	1.3256 ± 0.0708 kW	± 0.0879 kW
LSTM	P_{t+24h}	3.3151 ± 0.0480 kW	± 0.0596 kW	2.5420 ± 0.0551 kW	± 0.0684 kW
LSTM	SOC	5.2053 ± 0.0750 pp	± 0.0931 pp	3.5434 ± 0.1020 pp	± 0.1266 pp
GRU	P_{t+1}	2.0572 ± 0.0172 kW	± 0.0213 kW	1.1733 ± 0.0051 kW	± 0.0063 kW
GRU	P_{t+24h}	3.4222 ± 0.0347 kW	± 0.0431 kW	2.5700 ± 0.0750 kW	± 0.0932 kW
GRU	SOC	6.4779 ± 0.1932 pp	± 0.2399 pp	4.4485 ± 0.1591 pp	± 0.1976 pp
BiLSTM	P_{t+1}	2.2366 ± 0.0625 kW	± 0.0776 kW	1.3429 ± 0.0688 kW	± 0.0854 kW
BiLSTM	P_{t+24h}	3.2766 ± 0.0458 kW	± 0.0568 kW	2.4695 ± 0.0412 kW	± 0.0511 kW
BiLSTM	SOC	5.1630 ± 0.3126 pp	± 0.3882 pp	3.5552 ± 0.1587 pp	± 0.1971 pp

3. Results and Discussion

3.1. Forecasting Performance Analysis

RMSE and MAE were used to evaluate the forecasting performance of the LSTM, GRU, and BiLSTM models. Each model was trained five times using different random seeds while maintaining the same chronological training and testing partitions. The mean, standard deviation, and 95% confidence interval were calculated to assess the variability of model performance across repeated training runs. Table 4 presents the forecasting performance of the three models for the evaluated prediction targets.

For 15-minute-ahead solar-power prediction, GRU achieved the lowest RMSE and MAE, with values of 2.0572 ± 0.0172 kW and 1.1733 ± 0.0051 kW, respectively.

For 24-hour-ahead solar-power prediction, BiLSTM achieved the lowest RMSE and MAE, at 3.2766 ± 0.0458 kW and 2.4695 ± 0.0412 kW, respectively. For simulated SOC prediction, BiLSTM achieved the lowest RMSE of 5.1630 ± 0.3126 percentage points, whereas LSTM achieved the lowest MAE of 3.5434 ± 0.1020 percentage points.

These results indicate that no single recurrent architecture achieved the lowest error for every prediction target and metric. GRU performed best for short-term solar-power prediction, whereas BiLSTM achieved the lowest errors for 24-hour-ahead solar-power prediction. For simulated SOC prediction, the best-performing model depended on the evaluation metric. The standard deviations and confidence intervals provide additional information about variability across the five training runs. Figures 3 and 4 provide visual comparisons of the RMSE and MAE values reported in Table 4, respectively. The error bars represent ±1 standard deviation across the five training runs. Together, these figures illustrate that model performance varies according to the prediction target. GRU performed best for short-term solar-power prediction, while BiLSTM achieved the lowest errors for 24-hour-ahead solar-power prediction.

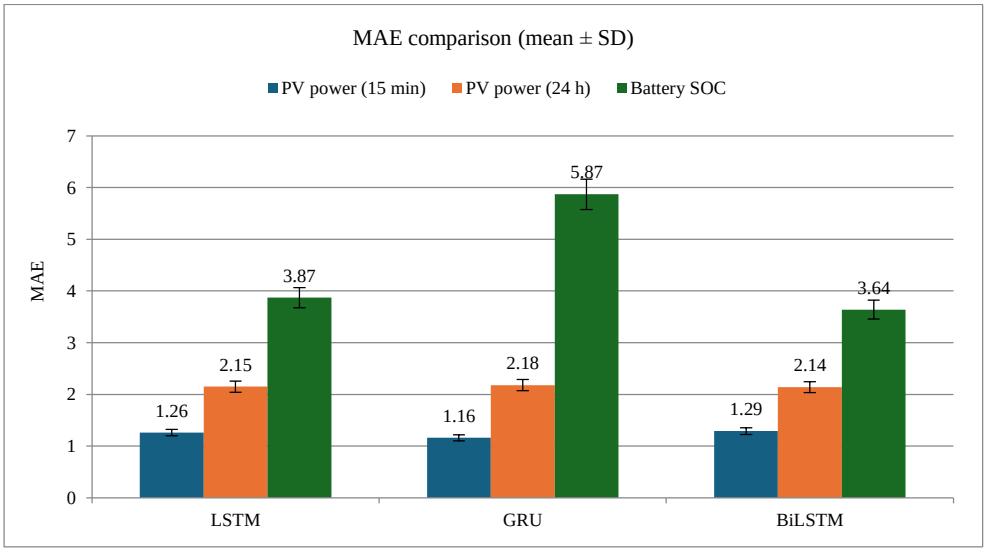

Fig. 3. Comparison of MAE values for the LSTM, GRU, and BiLSTM models across the evaluated prediction targets. Error bars indicate ±1 standard deviation across five training runs.

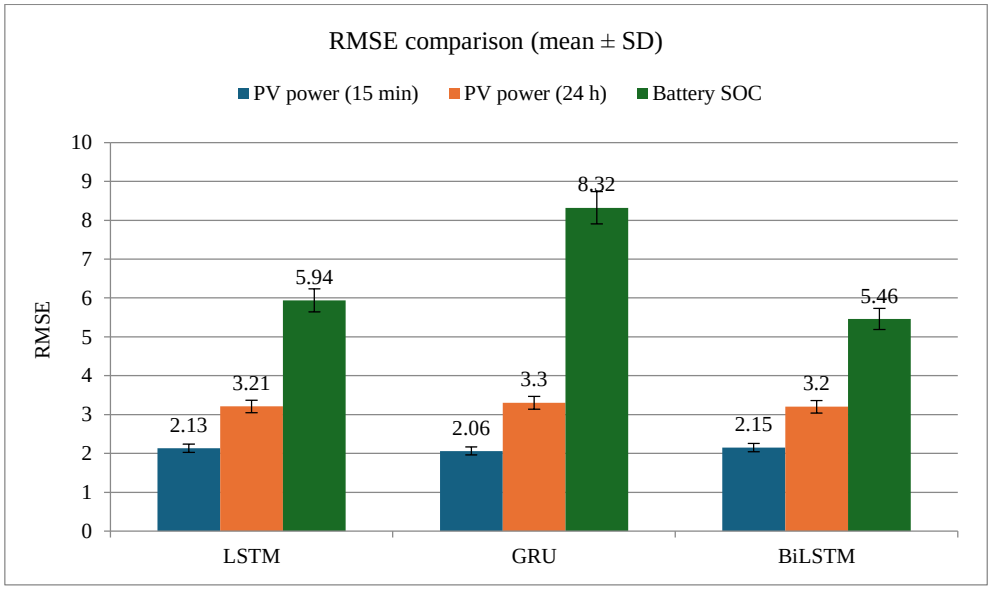

Fig. 4 Comparison of RMSE values for the LSTM, GRU, and BiLSTM models across the evaluated prediction targets. Error bars indicate ±1 standard deviation across five training runs.

For simulated SOC prediction, BiLSTM achieved the lowest RMSE, whereas LSTM achieved the lowest MAE. In Table 4, pp denotes percentage points. The 95% confidence interval columns report the half-width of the interval around the mean, calculated using the t-distribution with four degrees of freedom. Bold values indicate the lowest mean error for each output and metric. The proposed framework simultaneously predicts short-term solar power $P_{t+1,}$ 24-hour-ahead solar power P_{t+24h} , and simulated battery state of charge SOC. This multi-output structure enables solar-power forecasting and SOC estimation within a single framework. The temporal relationships between neighboring observations may be particularly useful for short-term solar-power forecasting. In contrast, uncertainty in future environmental conditions and variations in solar irradiance can make 24-hour-ahead forecasting more challenging. The evaluated models captured the overall variation in solar generation during the study period, although their prediction errors differed across the forecasting targets.

3.2. Actual and Predicted Solar Power Analysis

Figures 5 and 6 present the actual-versus-predicted solar-power results for the 15-minute-ahead and 24-hour-ahead forecasting tasks, respectively. The predictions from the LSTM, GRU, and BiLSTM models follow the general variation in solar-power generation, although discrepancies are observed during periods of rapid changes in power output. The differences between predicted and actual power are consistent with the forecasting errors reported in Table 4. These discrepancies may be associated with variations in irradiance and the nonlinear response of photovoltaic generation. Although solar-power and SOC predictions can provide useful information for battery scheduling, forecasting performance alone does not establish improvements in battery efficiency or reductions in grid-energy imports. Such benefits require separate evaluation using quantitative battery-management indicators.

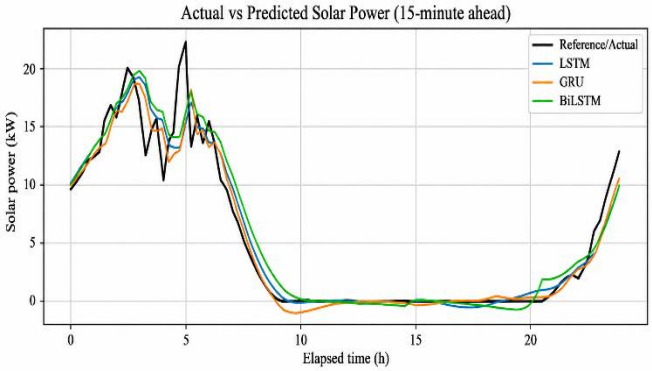

Fig. 5 Actual versus predicted solar power for the 15-minute-ahead forecasting task using the LSTM, GRU, and BiLSTM models

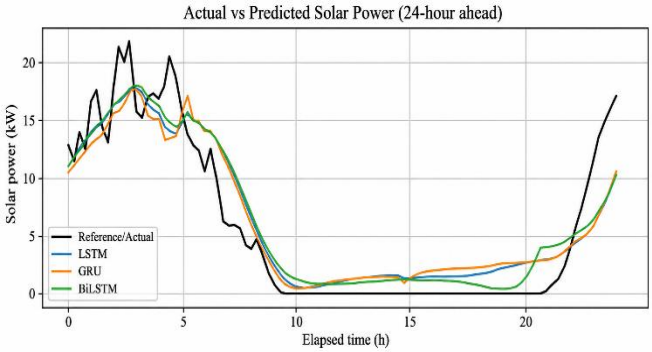

Fig. 6 Actual versus predicted solar power for the 24-hour-ahead forecasting task using the LSTM, GRU, and BiLSTM models

Table 5. Feature-based ablation results for the BiLSTM model across the three prediction targets

Ablation	Output	RMSE mean	RMSE SD	RMSE 95% CI	MAE mean	MAE SD	MAE 95% CI
AC power only	P_{t+1}	2.4832	0.0119	0.0148	1.5618	0.0653	0.0811
AC power only	P_{t+24h}	3.2307	0.0200	0.0248	2.3099	0.0230	0.0286
AC power only	SOC	5.3218	0.1798	0.2232	3.6767	0.2320	0.2880
Full features	P_{t+1}	2.2366	0.0625	0.0776	1.3429	0.0688	0.0854
Full features	P_{t+24h}	3.2766	0.0458	0.0568	2.4695	0.0412	0.0511
Full features	SOC	5.1630	0.3126	0.3881	3.5552	0.1587	0.1971
Without time	P_{t+1}	2.3644	0.0702	0.0872	1.4706	0.0640	0.0794
Without time	P_{t+24h}	3.3390	0.0499	0.0619	2.6061	0.0517	0.0642
Without time	SOC	5.1809	0.3206	0.3981	3.4907	0.2010	0.2495
Without weather	P_{t+1}	2.4685	0.0400	0.0497	1.5238	0.0406	0.0504
Without weather	P_{t+24h}	3.2084	0.0160	0.0199	2.2429	0.0675	0.0839
Without weather	SOC	5.1554	0.1070	0.1328	3.6028	0.1539	0.1911

Note: Values represent the mean, Standard Deviation (SD), and 95% confidence-interval half-width across five runs. Power errors are expressed in kW, whereas SOC errors are expressed in percentage points. Confidence intervals are reported as half-widths calculated using the t-distribution with four degrees of freedom.

3.3. Battery Scheduling Performance

A rule-based strategy-controlled battery charging and discharging according to solar generation, load demand, and SOC limits. Figure 7 shows the simulated SOC trajectory, which remained within the specified range of 20%-100%.

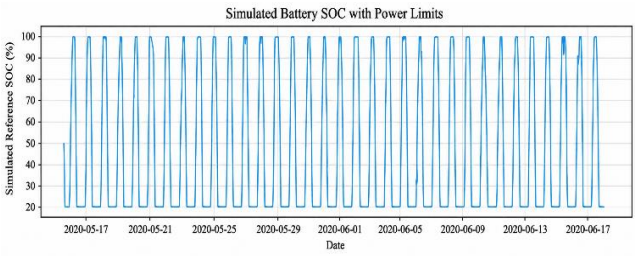

Fig. 7 Full-period simulated battery State-of-Charge (SOC) trajectory under the rule-based scheduling strategy, with SOC limits of 20% and 100%, respectively

Figure 7 presents the simulated battery SOC trajectory over the study period under the rule-based scheduling strategy. The SOC remained within the specified operating limits of 20%-100%.

However, the trajectory shows frequent transitions between the minimum and maximum SOC limits, indicating repeated saturation under the selected battery capacity, load, and scheduling assumptions.

Therefore, maintaining SOC within the specified limits does not, by itself, demonstrate improved battery efficiency or reduced grid-energy consumption.

3.4. Simulated Reference and Predicted SOC Analysis

Figure 8 compares simulated reference SOC with predictions from the LSTM, GRU, and BiLSTM models over a representative test interval. The predictions follow the general SOC trends, with differences during rapid transitions.

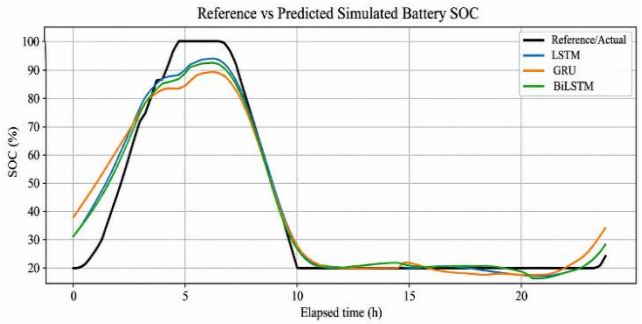

Fig. 8 Comparison of simulated reference SOC and predicted SOC obtained using the LSTM, GRU, and BiLSTM models over a representative test interval

3.5. Feature-based Ablation Study

To examine the contribution of the input features, a feature-based ablation study was conducted using the BiLSTM model. Four input configurations were evaluated: (i) full features, including AC power, irradiance, ambient temperature, module temperature, and hour of day; (ii) AC power and hour of day, excluding weather variables; (iii) AC power and weather variables, excluding the time feature; and (iv) AC power alone. Table 5 summarizes the RMSE and MAE results across five training runs.

Table 6. Comparison of related PV forecasting studies and the proposed framework

Study	Forecasting approach	Dataset/resolution	Forecasting target/horizon	Reported performance	Battery / SOC integration	Research gap relative to proposed work
Salman et al. [8]	CNN-LSTM-Transformer hybrid	Solar-power time-series dataset; resolution not specified	Solar-power forecasting	MAE = 0.551% for CNN-LSTM-TF with Nadam	No	Focuses on forecasting accuracy and optimizer selection; does not include SOC prediction or battery scheduling
Xiang et al. [11]	TCN-ECANet-GRU	Australian PV power station; 5-minute resolution	Short-term PV power; 3-, 6-, and 9-step horizons	RMSE = 0.0195, MAE = 0.0128, \(R^2 = 99.72\%\)	No	Uses an advanced hybrid forecasting model but does not jointly predict SOC or integrate battery scheduling

Alnejaili et al. [12]	Predictive PV-battery management	PV-battery off-grid energy system	Predictive energy management	Not directly comparable with the present forecasting metrics	Yes	Addresses PV-battery management, but not the same joint multi-output forecasting task.
Ma et al. [18]	Hybrid deep learning with transfer learning	PV forecasting dataset; details should be checked in source	Short-term PV power forecasting	Use source-reported metrics only; not directly comparable across datasets	No joint SOC scheduling	Uses transfer learning for forecasting without integrated SOC-based scheduling.
Tao et al. [21]	Transformer-variant PTFNet	Two public PV datasets; 15-minute resolution	Day-ahead PV power; 24-, 36-, and 40-hour horizons	Competitive performance reported across evaluated models; direct numerical comparison is not appropriate	No	PV forecasting-focused, without joint SOC prediction and battery scheduling.
Proposed framework	Multi-output BiLSTM	Rooftop PV dataset; 15-minute resolution	15-minute-ahead solar power, 24-hour-ahead solar power, and simulated reference SOC	Five-run RMSE, MAE, standard deviation, and 95% confidence intervals reported in this study	Yes-rule-based scheduling using predicted information and SOC limits	Integrates multi-output forecasting and SOC-based battery scheduling within a unified framework

Table 5 Feature-based ablation results for the BiLSTM model across the three prediction targets. Values represent the mean, Standard Deviation (SD), and 95% confidence-interval half-width across five runs. The results show that the contribution of input features varies across prediction targets. For 15-minute-ahead power prediction, the full feature set achieved the lowest RMSE and MAE, indicating the benefit of combining power, weather, and time information. For 24-hour-ahead prediction, the configuration without weather variables achieved the lowest RMSE and MAE, suggesting that the additional weather inputs did not improve performance in this dataset. For simulated SOC prediction, the configuration without weather variables achieved the lowest RMSE, while excluding the time feature produced the lowest MAE. Overall, no single feature configuration performed best across all outputs and metrics. These findings should be interpreted in the context of the dataset and the simulated SOC reference.

3.6. Comparison with Related Studies

Table 6 compares representative studies in solar PV forecasting in terms of model architecture, datasets, forecasting objectives, reported performance, and integration with battery or SOC management. Because the studies use different datasets, sampling intervals, forecasting horizons, and evaluation methods and their error values are not directly comparable. The comparison therefore emphasizes methodological characteristics and system integration. While many existing studies focus primarily on solar-power forecasting, the proposed framework jointly predicts short-term solar power, 24-hour-ahead solar power, and battery SOC, providing inputs for rule-based battery scheduling.

The main contribution is the integration of multi-output forecasting, SOC estimation, and rule-based scheduling rather than a new neural architecture or optimization algorithm. The best-performing model varies by target: GRU performs best for short-term power prediction, while BiLSTM performs best for 24-hour-ahead prediction. For SOC prediction, BiLSTM achieves the lowest RMSE, whereas LSTM achieves the lowest MAE. Further benchmarking and quantitative battery-management evaluation are needed to establish comparative advantages and practical energy-management benefits.

4. Conclusion

This study presented a multi-output deep learning framework for solar-power forecasting, battery State-of-Charge (SOC) estimation, and rule-based battery scheduling.

LSTM, GRU, and BiLSTM models were evaluated using 15-minute-resolution photovoltaic data to predict solar power 15 minutes and 24 hours ahead, together with a simulated reference SOC trajectory. Performance was assessed using RMSE and MAE over five independent training runs, with standard deviations and 95% confidence intervals used to characterize variability.

The results showed that model performance depended on the prediction target. GRU achieved the lowest RMSE and MAE for 15-minute-ahead forecasting (2.0572 kW and 1.1733 kW), while BiLSTM achieved the lowest errors for 24-hour-ahead forecasting (3.2766 kW and 2.4695 kW). For simulated SOC prediction, BiLSTM achieved the lowest RMSE (5.1630 percentage points), whereas LSTM achieved the lowest MAE (3.5434 percentage points). Thus, no single architecture performed best across all targets and metrics.

The forecasts were linked to a rule-based battery scheduling strategy operating within specified SOC limits. However, SOC was simulated rather than measured, and the results do not establish reductions in grid-energy imports, operating costs, or battery degradation. The findings therefore demonstrate forecasting performance and implementation of the specified scheduling rules, rather than proven improvements in energy-management efficiency.

Future work will validate the framework using measured battery SOC and longer-duration PV data, investigate feature contributions, and compare rule-based scheduling with optimization-based and model predictive control approaches. Evaluating renewable-energy utilization, grid imports, battery throughput, unmet demand, operating costs, and charge/discharge cycles will help establish its practical benefits.

References

[1] Hugo T.C. Pedro, and Carlos F.M. Coimbra, "Assessment of Forecasting Techniques for Solar Power Production with no Exogenous Inputs," *Solar Energy*, vol. 86, no. 7, pp. 2017-2028, 2012. [CrossRef] [Google Scholar] [Publisher Link]

[2] Cyril Voyant et al., "Machine Learning Methods for Solar Radiation Forecasting: A Review," *Renewable Energy*, vol. 105, pp. 569-582, 2017. [CrossRef] [Google Scholar] [Publisher Link]

[3] Sepp Hochreiter, and Jürgen Schmidhuber, "Long Short-Term Memory," *Neural Computation*, vol. 9, no. 8, pp. 1735-1780, 1997. [CrossRef] [Google Scholar] [Publisher Link]

[4] Yusen Wang, Wenlong Liao, and Yuqing Chang, "Gated Recurrent Unit Network-based Short-Term Photovoltaic Forecasting," *Energies*, vol. 11, no. 8, pp. 1-14, 2018. [CrossRef] [Google Scholar] [Publisher Link]

[5] Mike Schuster, and Kuldip K. Paliwal, "Bidirectional Recurrent Neural Networks," *IEEE Transactions on Signal Processing*, vol. 45, no. 11, pp. 2673-2681, 1997. [CrossRef] [Google Scholar] [Publisher Link]

[6] Luca Massidda, Fabio Bettio, and Marino Marrocu, "Probabilistic Day-Ahead Prediction of PV Generation. A Comparative Analysis of Forecasting Methodologies and of the Factors Influencing Accuracy," *Solar Energy*, vol. 271, pp. 1-16, 2024. [CrossRef] [Google Scholar] [Publisher Link]

[7] Kadír Olcay, Samet Gíray Tunca, and Mustafa Aríf Özgür, "Forecasting and Performance Analysis of Energy Production in Solar Power Plants using Long Short-Term Memory (LSTM) and Random Forest Models," *IEEE Access*, vol. 12, pp. 103299-103312, 2024. [CrossRef] [Google Scholar] [Publisher Link]

[8] Diaa Salman et al., "Hybrid Deep Learning Models for Time Series Forecasting of Solar Power," *Neural Computing and Applications*, vol. 36, no. 16, pp. 9095-9112, 2024. [CrossRef] [Google Scholar] [Publisher Link]

[9] Khaled Ferkous et al., "A Novel Learning Approach for Short-Term Photovoltaic Power Forecasting - A Review and Case Studies," *Engineering Applications of Artificial Intelligence*, vol. 133, 2024. [CrossRef] [Google Scholar] [Publisher Link]

[10] Hao Zhen et al., "Photovoltaic Power Forecasting based on GA Improved Bi-LSTM in Microgrid Without Meteorological Information," *Energy*, vol. 231, 2021. [CrossRef] [Google Scholar] [Publisher Link]

[11] Xiuli Xiang et al., "A Short-Term Forecasting Method for Photovoltaic Power Generation based on the TCN-ECANet-GRU Hybrid Model," *Scientific Reports*, vol. 14, no. 1, pp. 1-12, 2024. [CrossRef] [Google Scholar] [Publisher Link]

[12] Tareq Alnejaili, Sami Labdai, and Larbi Chrifi-Alaoui, "Predictive Management Algorithm for Controlling PV-Battery Off-Grid Energy System," *Sensors*, vol. 21, no. 19, pp. 1-16, 2021. [CrossRef] [Google Scholar] [Publisher Link]

[13] Oussama Khouili et al., "Evaluating the Impact of deep Learning Approaches on Solar Photovoltaic Forecasting: A Systematic Review," *Energy Strategy Reviews*, vol. 59, pp. 1-18, 2025. [CrossRef] [Google Scholar] [Publisher Link]

[14] Sameh Mahjoub et al., "Control and Implementation of an Energy Management Strategy for a PV-Wind-Battery Microgrid based on an Intelligent Prediction Algorithm of Energy Production," *Energies*, vol. 16, no. 4, pp. 1-26, 2023. [CrossRef] [Google Scholar] [Publisher Link]

[15] Alessandra Parisio, Evangelos Rikos, and Luigi Glielmo, "A Model Predictive Control Approach to Microgrid Operation Optimization," *IEEE Transactions on Control Systems Technology*, vol. 22, no. 5, pp. 1813-1827, 2014. [CrossRef] [Google Scholar] [Publisher Link]

[16] Jonathan Dumas et al., "Deep Learning based Multi-Output Quantile Forecasting of PV Generation," *2021 IEEE Madrid PowerTech*, Madrid, Spain, pp. 1-6, 2021. [CrossRef] [Google Scholar] [Publisher Link]

[17] Daniel Vázquez Pombo et al., "Increasing the Accuracy of Hourly Multi-Output Solar Power Forecast with Physics-Informed Machine Learning," *Sensors*, vol. 22, no. 4, pp. 1-20, 2022. [CrossRef] [Google Scholar] [Publisher Link]

[18] Tiandong Ma et al., "Short-term Photovoltaic Power Forecasting based on a New Hybrid Deep Learning Model Incorporating Transfer Learning Strategy," *Global Energy Interconnection*, vol. 7, no. 6, pp. 825-835, 2024. [CrossRef] [Google Scholar] [Publisher Link]

[19] Haixu Wu et al., "Autoformer: Decomposition Transformers with Auto-Correlation for Long-Term Series Forecasting," *Advances in Neural Information Processing Systems*, vol. 34, pp. 22419-22430, 2021. [Google Scholar] [Publisher Link]

[20] Haoyi Zhou et al., "Informer: Beyond Efficient Transformer for Long Sequence Time-Series Forecasting," *Proceedings of the AAAI Conference on Artificial Intelligence*, vol. 35, no. 12, pp. 11106-11115, 2021. [CrossRef] [Google Scholar] [Publisher Link]

[21] Kejun Tao et al., "Operational Day-Ahead Photovoltaic Power Forecasting based on Transformer Variant," *Applied Energy*, vol. 373, 2024. [CrossRef] [Google Scholar] [Publisher Link]